

Discovering vanishing objects in POSS I red images using the Virtual Observatory

Enrique Solano,^{1,2*} B. Villarroel,^{3,4} C. Rodrigo^{1,2}

¹*Centro de Astrobiología (CAB), CSIC-INTA, Camino Bajo del Castillo s/n, E-28692, Villanueva de la Cañada, Madrid, Spain*

²*Spanish Virtual Observatory*

³*Nordita, KTH Royal Institute of Technology and Stockholm University, Roslagstullsbacken 23, SE-106 91 Stockholm, Sweden*

⁴*Instituto de Astrofísica de Canarias, Avda Vía Láctea S/N, La Laguna, E-38205, Tenerife, Spain*

Accepted 2022 May 31. Received 2022 May 03; in original form 2022 March 08

ABSTRACT

In this paper we report a search for vanishing sources in POSS I red images using Virtual Observatory archives, tools and services. The search, conducted in the framework of the VASCO project, aims at finding POSS I (red) sources not present in recent catalogues like Pan-STARRS DR2 (limiting magnitude $r=21.4$) or *Gaia* EDR3 (limiting magnitude $G=21$). We found 298 165 sources visible only in POSS I plates, out of which 288 770 had a crossmatch within 5 arcsec in other archives (mainly in the infrared), 189 were classified as asteroids, 35 as variable objects, 3 592 as artefacts from the comparison to a second digitization (Supercosmos), and 180 as high proper motion objects without information on proper motion in *Gaia* EDR3. The remaining unidentified transients (5 399) as well as the 172 163 sources not detected in the optical but identified in the infrared regime are available from a Virtual Observatory compliant archive and can be of interest in searches for strong M-dwarf flares, high-redshift supernovae, asteroids, or other categories of unidentified red transients. No point sources were detected by both POSS-I and POSS-II before vanishing, setting the rate of failed supernovae in the Milky Way during 70 years to less than one in one billion.

Key words: astronomical data bases: surveys – astronomical data bases: virtual observatory tools – transients

1 INTRODUCTION

Transients can be defined as astrophysical phenomena whose duration is significantly lower than the typical timescale of the stellar and galactic evolution (from seconds to years in contrast to millions or billions of years). Supernovae, novae, gamma-ray bursts, ..., are some examples of transient events.

While most of the modern surveys have developed robust and well tested facilities to discover transients (ASAS (Pojmanski 1997), OGLE (Udalski et al. 2015), ZTF (Bellm et al. 2019) or *Gaia* (Gaia Collaboration et al. 2021), to name a few), the same level of attention is not paid to vanishing events, that is, objects detected in old surveys but that are not identified in more recent ones. In this context, vanishing refers both to known types of objects faded below the detection limits (e.g. large amplitude variables) as well to unknown physical phenomena non predicted before. Objects that do not appear in the same position because they have moved in the sky (e.g. solar system objects) do not belong to this category.

VASCO¹ (Vanishing and Appearing Sources during a Century of Observations) is a project to search for vanishing and appearing sources using existing survey data. Examples of exceptional astrophysical transients found with VASCO are given in Villarroel et al. (2020b). VASCO also runs a citizen science project that investigates

150 000 candidates visually (Villarroel et al. 2020a). This paper, conceived in the frame of the VASCO project, aims at performing an automated search for vanishing object using the digitized plates of the First Palomar Sky Survey (POSS I) and the Pan-STARRS (DR2) and *Gaia* EDR3 catalogues taking advantage of Virtual Observatory (VO) tools and services².

POSS I was conducted between 1949–1956 (99 per cent of the plates) and 1956–1958 (1 per cent of the plates) using the 48-inch Oschin Schmidt telescope at Mount Palomar in southern California (Minkowski & Abell 1963). The survey covers the entire sky north of -45 deg declination and was carried out using photographic plates, later converted into a digital format. In order to obtain colour information, each region of the sky was photographed twice, once using a blue sensitive Kodak 103a-O plate, and once with a red sensitive Kodak 103a-E plate, peaking at $\sim 4 100$ and $\sim 6 400$ Å, respectively³. The limiting photographic magnitudes of the blue and red plates are 21.1 and 20.0 mag, respectively.

In this paper we made use of the digitization of the POSS I red plates available from the Digitized Sky Survey from ESO⁴ and pro-

² <https://www.ivoa.net/>

³ https://authors.library.caltech.edu/31250/1/Palomar_Observatory_Sky_Atlas.pdf

⁴ <http://archive.eso.org/dss/dss/>

* E-mail: esm@cab.inta-csic.es

¹ <https://vasconsite.wordpress.com/>

duced at the Space Telescope Science Institute through its Guide Star Survey group⁵.

The Panoramic Survey Telescope and Rapid Response System (Pan-STARRS⁶) is a system for wide-field astronomical imaging developed and operated by the Institute for Astronomy at the University of Hawaii. Pan-STARRS1 (PS1) is the first part of Pan-STARRS. PS1, located at Haleakala Observatory, started operation in 2010 and have surveyed the sky in five bands (g,r,i,z,y) at declinations higher than -30 deg using a 1.8 meter telescope and a 1.4 Gigapixel camera. The PS1 Second Data Release (DR2) survey contains almost 2 billion objects and was released on January 28, 2019. PS1 (DR2) was queried using the corresponding Virtual Observatory ConeSearch service⁷.

Gaia is a European space mission providing astrometry, photometry and spectroscopy of more than 1 500 million stars in the Milky Way. Also data for significant samples of extragalactic and Solar system objects are made available. Photometric information is provided in three bands: G , G_{BP} and G_{RP} with a limiting magnitude of $G \sim 21$ mag⁸. *Gaia* EDR3 (Gaia Collaboration et al. 2021) is based on data collected between 25 July 2014 and 28 May 2017, spanning a period of 34 months. *Gaia* EDR3 data were gathered through the Vizier (Ochsenbein et al. 2000) service.

This article is organized as follows: In Sect. 2, we describe the methodology followed to identify candidates to vanishing objects while, in Sect. 3 we assess the different hypothesis to explain the physical nature of those candidates. After Sect. 4 and Sect. 5 where we report the discovery of a brown dwarf candidate in POSS I and give an estimation of the number of vanishing stars, respectively, we summarized the main results of the paper in Sect. 6. A brief description of the Virtual Observatory compliant archive than contains detailed information on the candidates is given in the Appendix.

2 CANDIDATE SELECTION

We built a VO-workflow consisting in the following steps:

- Sky tessellation: To avoid memory overflow problems associated to the data processing of large volumes of data, we made use of the scripting capabilities of Aladin⁹ (Bonnarel et al. 2000; Boch & Fernique 2014), to tessellate the sky covered by POSS I in circular regions of 30 arcmin radius.

- Source extraction: For each one of these regions, we run SExtractor (Bertin & Arnouts 1996) to build a catalogue of sources. To minimize the number of false sources in noisy images and detect only sources well above the noise level, the DETECT_THRESH parameter was set to 5 and only sources with SNR_WIN>30 and FLAG= 0 were kept.

- Cross-matching: We made use of the CDSSkymatch functionality implemented in STILTS¹⁰ (Taylor 2006) to cross-match the catalogue of sources obtained in the previous step with the *Gaia* EDR3 and Pan-STARRS DR2 catalogues. Sources in the SExtractor catalogue not having counterparts either in *Gaia* or Pan-STARRS in a 5 arcsec radius were kept. The adopted radius is a good compromise

⁵ <http://gsss.stsci.edu/Catalogs/Catalogs.htm>

⁶ <https://panstarrs.stsci.edu/>

⁷ <http://gsss.stsci.edu/webservices/vo/CatalogSearch.aspx?&CAT=PS1V30BJECTS&RA=&DEC=&SR=>

⁸ <https://www.cosmos.esa.int/web/gaia/earlydr3>

⁹ <https://aladin.u-strasbg.fr/>

¹⁰ <http://www.star.bris.ac.uk/~mbt/stilts/>

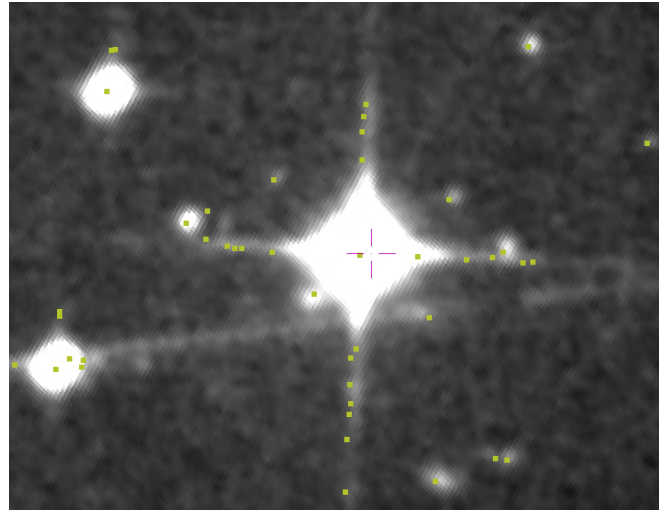


Figure 1. Example of a POSS I image with a bright source showing diffraction spikes. Green squares correspond to USNO B-1.0 sources.

to ensure that not many high proper motion were left out while, at the same time, avoiding an unmanageable number of false positives.

- Spikes' removal: Spurious detections appearing on the diffraction spikes of very bright sources in POSS I images must be identified and removed. After some trial and error, we implemented the following empirical procedure to remove them:

- For each SExtractor source we look for counterparts in the USNO B-1.0¹¹ (Monet et al. 2003) in a circular region of 90 arcmin radius.

- SExtractor sources having a USNO counterpart fulfilling any of the following two conditions were rejected.

- R_{mag1} or $R_{mag2} < 12.4$

- R_{mag1} or $R_{mag2} < -0.09 \times d + 15.3$

where d is the angular separation in arcsec between the SExtractor and the USNO B-1.0 source and R_{mag1} and R_{mag2} are the USNO magnitudes in the red band at two different epochs. (Fig. 1).

- Other artefacts' removal: Morphometric parameters like the full width at half maximum (FWHM) or the elongation were used to clean the SExtractor catalogue from spurious sources. For each image, we computed the median and the absolute deviation of the median of the FWHM and the elongation of the sources in order to remove sources deviating more than 2σ from the median values (Fig. 2). Additionally, we also applied the following filtering conditions:

- $SPREAD_MODEL > -0.002$

- $2 < FWHM < 7$

- $ELONGATION < 1.3$

- $\text{abs}((X_{MAX_IMAGE} - X_{MIN_IMAGE}) - (Y_{MAX_IMAGE} - Y_{MIN_IMAGE})) < 2$

- $X_{MAX_IMAGE} - X_{MIN_IMAGE} > 1$

- $Y_{MAX_IMAGE} - Y_{MIN_IMAGE} > 1$

$SPREAD_MODEL$ is a SExtractor parameter intended to be a point/extended source classifier. By construction, $SPREAD_MODEL$ is close to zero for point sources, positive for extended sources

¹¹ <https://cdsarc.cds.unistra.fr/viz-bin/cat/I/284>

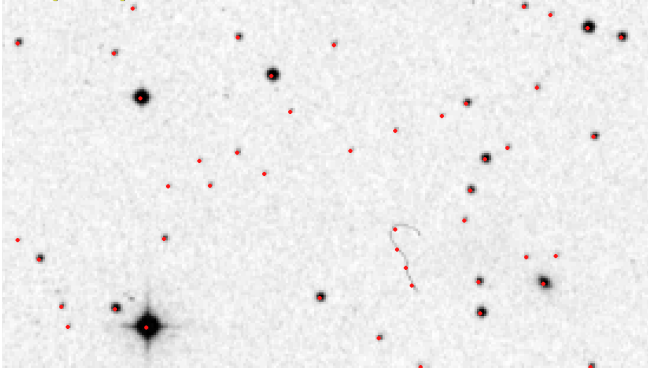


Figure 2. Example of a POSS I image showing a cane-shaped artefact (located at the centre-right of the image), which is removed from the SExtractor catalogue according to its anomalous values of FWHM and elongation. SExtractor sources are overlaid as red dots.

(galaxies), and negative for detections smaller than the PSF, such as cosmic ray hits. $XMAX/XMIN/YMAX/YMIN$ indicate the maximum/minimum x/y coordinate among detected pixels. Our condition forces the source to be larger than one pixel and of similar size in both directions.

- Identification of high proper motion objects: The ~ 60 yr time baseline between the POSS I images and *Gaia* and Pan-STARRS leads that objects with proper motions typically higher than 80 mas yr^{-1} may lie outside our 5 arcmin radius searches becoming, thus, potential candidates. To identify and remove them from the list of candidates, we made use of the observing epoch of the POSS I images (keyword: EPOCH).

For each one of the SExtractor sources fulfilling all the conditions described in the previous steps, we cross-matched them with *Gaia* EDR3 in a 180 arcmin radius, keeping all the counterparts in that radius. For these *Gaia* counterparts, we kept those having proper motion information, which was used to correct the position of the *Gaia* counterparts to the POSS I epoch. The adopted epoch for *Gaia* was J2016.0. SExtractor sources having a *Gaia* counterpart (corrected at POSS I epoch) at less of 5 arcsec were flagged as high proper motion sources and, therefore, removed from the list of candidates (Fig. 3).

- Concatenation: The lists of sources fulfilling all the previous steps were concatenated into a single table and removed duplicated instances as tessellated images may overlap. After all this process, we ended up with a list of 298 165 POSS I sources not seen either in *Gaia* EDR3 or Pan-STARRS DR2.

3 ANALYSIS

In the previous section we obtained a total of 298 165 potential sources that do not have counterparts either in Pan-STARRS DR2 or *Gaia* EDR3 within a certain distance (5 arcsec). In what follows we will study the possible nature of these sources.

- Objects not present either in *Gaia* EDR3 or Pan-STARRS but present in other astronomical surveys. To check this possibility we looked for counterparts in the catalogues available from the *CDS* Upload X-match utility implemented in TOPCAT (Taylor 2005) and from IRSA (Neowise, PTF). These searches were complemented

with a search in the catalogues available from VOSA (Bayo et al. 2008)¹². Sources with counterparts at less than 5 arcsec in any of the queried photometric catalogues were removed from our list of candidates to vanishing objects.

These searches significantly reduced the number of candidates (from 298 165 to 9 395). A significant number (~ 59 per cent) of the identified sources were visible in infrared catalogues (Neowise, CatWISE2020, unWISE, and the infrared catalogues included in VOSA) but not in the optical (KIDS, Skymapper, and the optical catalogues included in VOSA) or the ultraviolet (GALEX). The sources detected in the infrared but not in the optical/ultraviolet are available from the online archive (see Appendix).

We also queried the Astrographic Catalogue (Urban et al. 1998) to look for observations previous to POSS I epoch finding no results.

- Asteroids: The typical exposure time of the POSS I red images (45-60 min) and the mean daily motion of Main Belt asteroids ($0.1\text{-}0.3 \text{ deg d}^{-1}$, larger for nearer asteroids) make that most of these objects leave a stripe on the POSS I red images (Fig. 4). Although due to its elongated shape, most of them are discarded in the search procedure, very slow asteroids mimicking point-like sources could escape from the filtering criteria. In order to also discard these sources we made use of the SkyBoT¹³ VO service (Berthier et al. 2006) to look for known asteroids lying in the POSS I field of view at the time when the image was observed. Sources lying at less than 1 arcmin from the predicted position of the asteroid were removed. 189 asteroids were found leaving us with 9 206 (9 395-189) candidates.

- Stellar variability: It might happen that our candidates are not visible either in *Gaia* EDR3, Pan-STARRS or other catalogues simply because they are large amplitude variable objects reaching their faintest magnitudes at the time when they were observed in those surveys. *Gaia* EDR3 and Pan-STARRS are deeper surveys than POSS I but, how much deeper are they? In order to estimate the limiting magnitude of our POSS I candidates in the *Gaia* EDR3 and Pan-STARRS photometric systems, we randomly selected 100 candidates. Centred on each one of them, we cutout a POSS I image of 15×15 arcmin radius and, using SExtractor, compiled the sources present in them. A total of $\sim 22\,000$ sources were obtained. These sources were cross-matched with *Gaia* EDR3 and Pan-STARRS with a 5 arcsec search radius to look for counterparts in these catalogues. We got 19 804 and 20 784 counterparts in *Gaia* EDR3 and Pan-STARRS, respectively. Fig. 5 shows the distribution of the *Gaia* EDR3 (G band) and Pan-STARRS (r band) magnitudes. We see how completeness is reached for POSS I sources at $G = 18.5$ in *Gaia* EDR3 and $r = 19$ in Pan-STARRS. The limiting magnitude of *Gaia* EDR3 ($G = 21$) (Gaia Collaboration et al. 2021) and Pan-STARRS ($r = 21.8$)¹⁴ imply that, for a source not to be visible in *Gaia* EDR3 and Pan-STARRS, the drop in magnitude should be larger than 2.5 mag approximately.

Flare stars are objects with spectral types later than late-K that can undergo unpredictable dramatic increases in brightness for a few minutes or hours before returning to their quiescent state (e.g. Greiner & Motch 1995). The relatively little time spent at the brightest magnitude (the flare duty cycle for M dwarfs is found to increase from 0.02% for early M dwarfs to 3% for late M dwarfs (Hilton et al. 2010).

¹² The list of catalogues consulted by VOSA can be found at <http://svo2.cab.inta-csic.es/theory/vosa/help/star/credits/>

¹³ <https://vo.imcce.fr/webservices/skybot/>

¹⁴ <https://panstarrs.stsci.edu/>

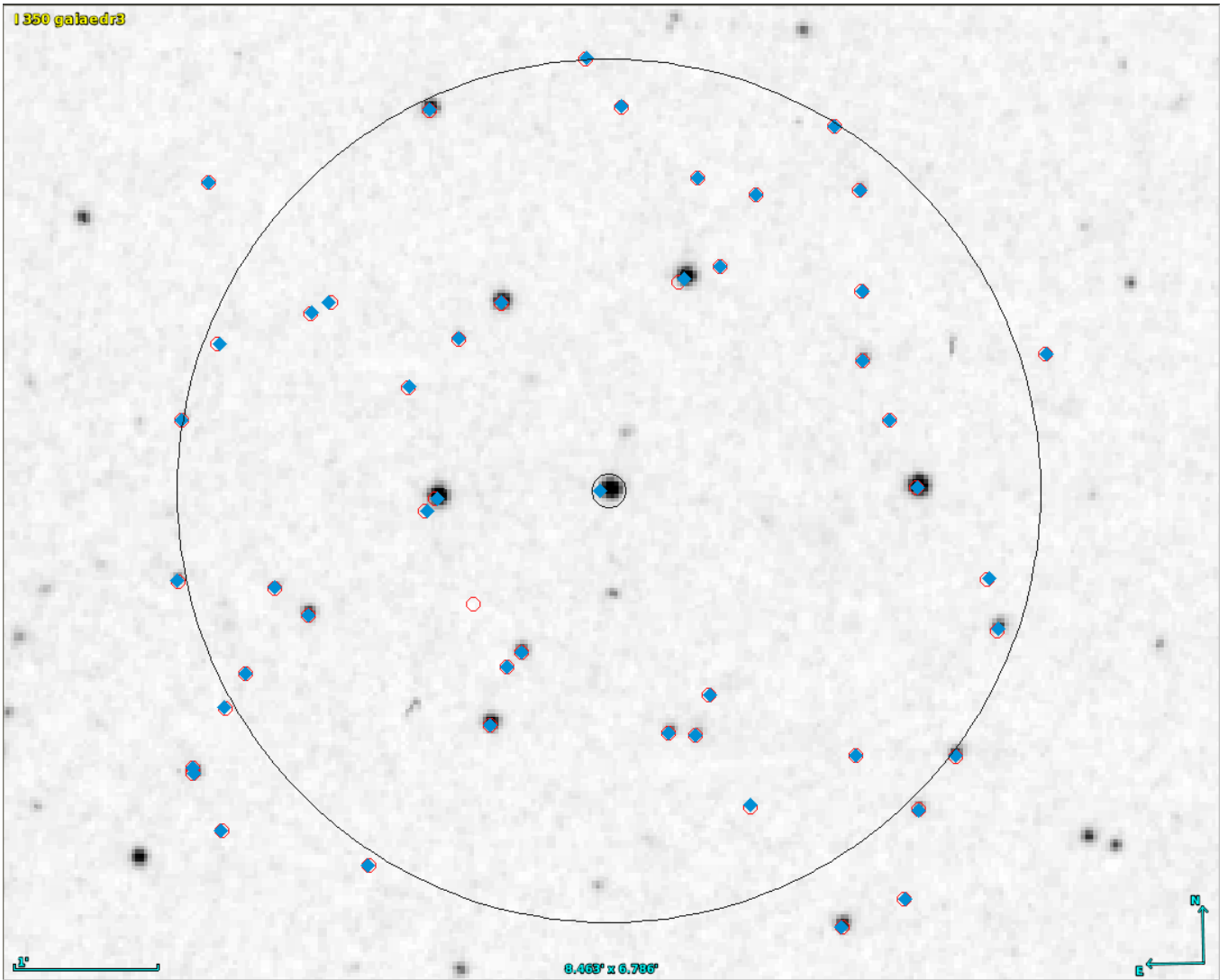


Figure 3. Example of a high proper motion source (centre of the image). Red open circles represent Gaia counterparts at J2016.0 epoch. Solid blue diamonds indicate the position of the same sources at the POSS I epoch. The isolated red circle at lower left of centre really coincides with the POSS I source at the centre of the image if the POSS I epoch is considered (blue diamond inside the inner circle). The outer and inner black circles correspond to the 3 arcmin and 5 arcsec search radius, respectively.

The duty cycle is defined as the percentage of time in a entire period of observation where flares occur), their unpredictable occurrence together with the fact that M stars are the most numerous objects in the galaxy (Cifuentes et al. 2020), make flare stars good candidates to explain the nature of, at least, a significant part of our sources. Nevertheless, differences in the type of data used to estimate the frequency of flares – time-resolved photometric (Kowalski et al. 2009) or spectroscopic (Hilton et al. 2010) surveys –, in the wavelength range (near UV, optical), in the magnitudes used to count the number of flares (duty cycle, flares per hour), in the parameters used for flare identification – *flare variability index* (Kowalski et al. 2009), *flare line index* (Hilton et al. 2010) –, or the existing correlation with spatial distribution, spectral type or age – begin more frequent close to the Galactic plane, at later spectral types and at younger ages (Hilton et al. 2010) –, makes it quite difficult to give a realistic estimation of the number of flaring objects among our final list of unidentified transients.

Other (although less numerous) types of stellar objects triggering large amplitude variations are, for instance, LBVs (van Genderen 2001), FUORs (Hartmann & Kenyon 1996), RCB stars (Benson et al. 1994), ILRTs (Cai et al. 2021), K giants (Tang et al. 2010), cataclysmic objects like novae or pulsating variables like Miras (Reid & Goldston 2002), RV Tau stars (de Ruyter et al. 2005) or Cepheids (Klagyivik & Szabados 2009). Other potential types of variable objects can be found in Byrne & Fraser (2022). Moreover, extragalactic transients that can be associated to rare blazars or accretion outbursts in active galactic nuclei (Lawrence et al. 2016) or highly variable quasars or microlensing events (Nagoshi et al. 2021) can also contribute.

In order to assess whether our candidates to vanishing objects were already known variable objects, we searched for them in the International Variable Star Index¹⁵ (Watson et al. 2006) and in the

¹⁵ <https://cdsarc.cds.unistra.fr/viz-bin/cat/B/vsx>

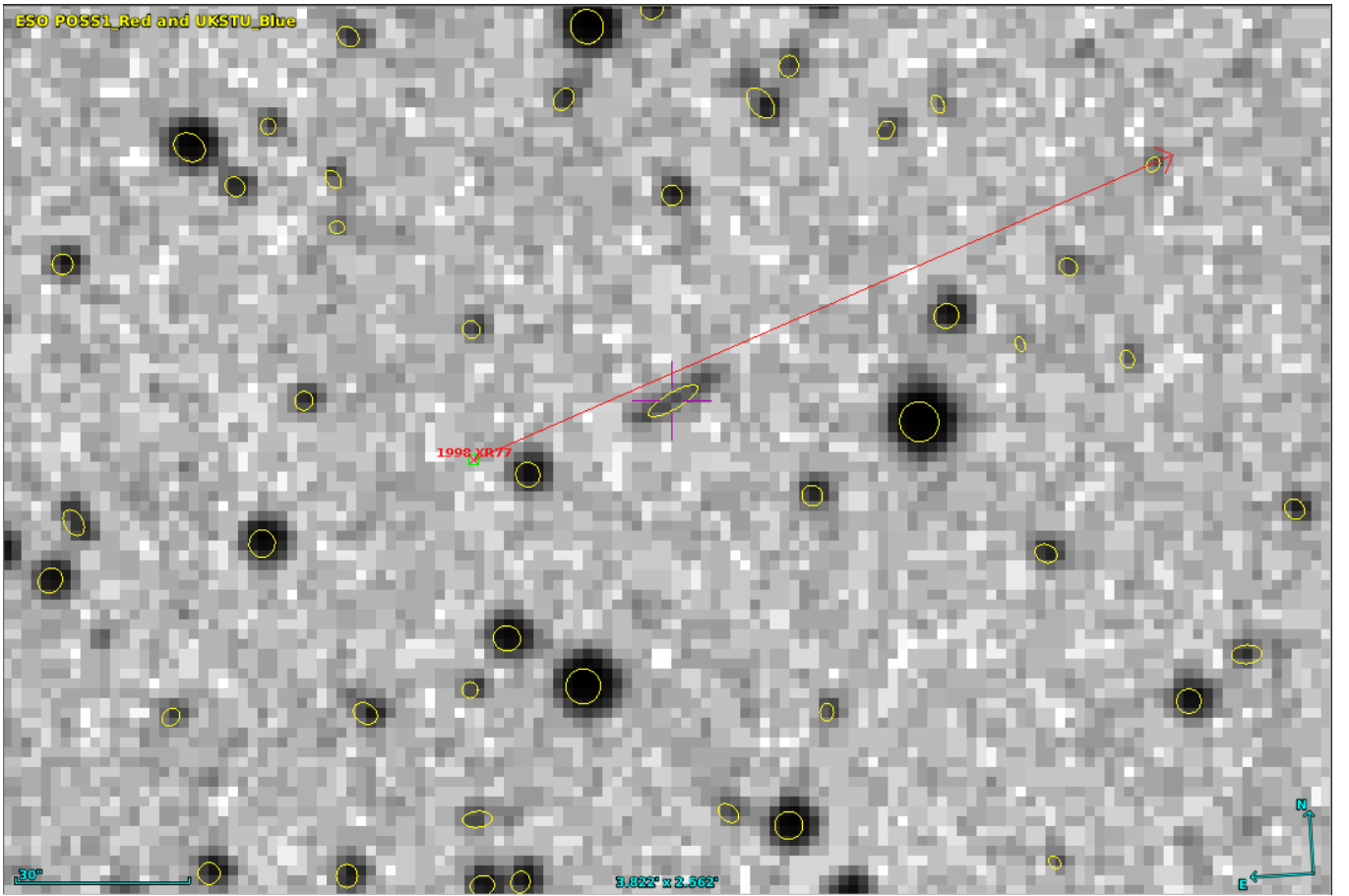


Figure 4. Detection of the asteroid 1998 XR77 (centre of the image). Its elongated, striped shape is clearly visible. The predicted position by Skybot (~ 35 arcsec south-east from the real position) as well as its trajectory are plotted in red. Yellow shapes indicate the sources identified by SExtractor.

Transient Name Server¹⁶. In both cases no counterparts were found at less than 5 arcsec. We also queried the PTF object catalogue available at IRSA¹⁷ finding 62 counterparts, out of which 35 were flagged as good ($ngoodobs > 0$). This reduced the number of candidates to 9 171 (9 206-35).

- Supernovae, hypernovae and failed supernovae: Much less frequent but still possible is that some of our candidates may be ascribed to explosions of very luminous supernovae and hypernovae. If these objects are hosted in very faint galaxies, they will be visible just at the time of explosion keeping no track in images taken subsequently. ASASSN-15lh / SN 2015L, the most luminous supernovae observed so far thought to be originated by the tidal disruption of a star when crossing the tidal radius of a supermassive black hole (Leloudas et al. 2016), or GRB171205A a hypernovae caused by the explosion of a very massive star (Izzo et al. 2019) could be examples of the objects belonging to this category.

Failed supernovae, on its part, have been proposed to explain the absence of Type IIP core-collapse supernovae arising from progenitors above $17 M_{\odot}$. In this scenario, the stellar cores will collapse directly to form a black hole without producing the

explosion of the star (Byrne & Fraser 2022). As for supernovae and hypernovae, failed supernovae occurring at POSS-I epoch will not be visible in modern archives. Different candidates to failed supernovae have been proposed in the literature (Kochanek et al. 2008; Reynolds et al. 2015; Neustadt et al. 2021) but the real nature of these objects is still far from being confirmed.

- Artefacts: Could artefacts resemble point-like sources and, thus, escape from our morphometric criteria? Small dust particles sticking to the plate during exposures or microspots originated over the years may produce this type of point-like features (Villarreal et al. 2020b). Clearly, a human inspection of the POSS I plates could solve the problem. However, the original plates of old sky surveys are treated like gold and accessing those plates is extraordinarily rare. An alternative to remove candidates artefacts originated during the scanning process is to compare the images digitized at STSCI with those digitized by SuperCosmos¹⁸. The comparison was carried out using the Table Access Protocol (TAP) service implemented in the GAVO Data Centre¹⁹. Candidates having a counterpart in the SuperCosmos digitization at less than 5 arcsec were kept. After this comparison, 5 579 candidates still remain.

¹⁶ <https://www.wis-tns.org/>

¹⁷ <https://irsa.ipac.caltech.edu/cgi-bin/Gator/nph-scan?mission=irsa&submit=Select&projshort=PTF>

¹⁸ <https://www.roe.ac.uk/ifa/wfau/cosmos/scosmos.html>

¹⁹ <http://dc.zah.uni-heidelberg.de/tap>

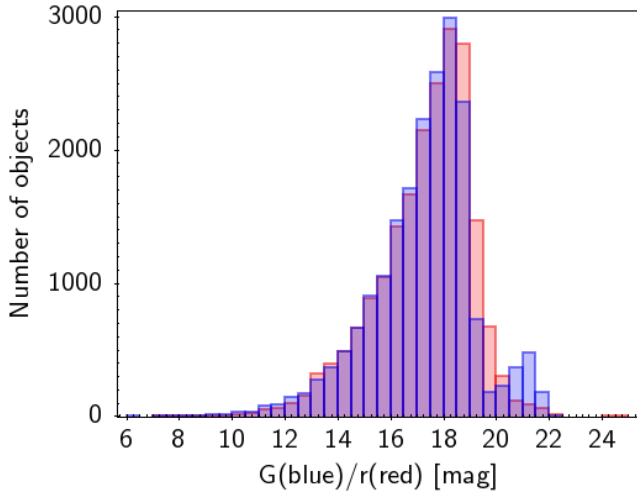


Figure 5. Distribution of the *Gaia* EDR3 (blue) and Pan-STARRS (red) magnitudes of a randomly selected sample of POSS I sources. Limiting magnitudes of POSS I sources at *Gaia* EDR3 and Pan-STARRS are $G=18.5$ and $r=19$, respectively.

- Wrong astrometry. If the POSS I red images from where the candidates to vanishing objects were extracted have poor astrometry, then, the extracted sources will appear displaced from the *Gaia* EDR3 and Pan-STARRS positions being, thus, flagged as candidates.

To check this possibility, we randomly selected a subsample of $\sim 400\,000$ sources extracted from POSS I images, sources that were crossmatched with *Gaia* EDR3. The mean and median values for the differences in position were 0.97 and 0.91 arcsec, respectively with an standard deviation of 0.5 arcsec. Thus, we can conclude that wrong astrometry cannot explain the number of candidates to vanishing objects we have found.

- Technosignatures: Technosignatures can be defined as properties or effects that cannot be ascribed to natural phenomena and, thus, may indicate an artificial origin (e.g. artificial communication lasers, Dyson spheres and megastructures. In particular, the latter two could make a dim or even vanish entirely the star). The role of vanishing stars in searches for technosignatures were first presented in Villarroel et al. (2016). A general overview describing the possibilities of technosignature searches in time-domain astronomy is given in Davenport (2019) while concrete examples can be found in Villarroel et al. (2020b). Human satellites at the geostationary orbit could be argued as a possibility to explain the glints found in POSS I images, glints that could be caused by reflections of the Sun. This glints would be bright, have a PSF-like shape and short duration (Villarroel et al. 2022). However, we remind the reader that the launch of the first satellite happened in 1957, when most of the POSS I survey was already completed.

- High proper motion objects without proper motion information in *Gaia* EDR3. Not all sources included in *Gaia* EDR3 have associated an estimation of their proper motion. If this is the case and the object has a significant proper motion, it could be wrongly flagged as candidate to vanishing object. In order to identify these fast-moving objects, we carried out a visual inspection using Aladin. First, we made use of the proper motion information available in Simbad for objects at small angular distances from our candidates. This way we discarded 178 objects (Fig. 6). For the remaining 5 401 (5 579-

178) candidates we looked for sources at close angular distances in catalogues with different time coverage (2MASS, SDSS, UKIDSS, ZTF) aiming at finding a clear linear displacement between images (Fig. 7). After this visual inspection we ended up with a final list of 5 399 candidates to vanishing objects. A flowchart summarising the selection and analysis process is shown in Fig. 8. The spatial distribution in galactic coordinates of the final list of candidates as well the distribution of their magnitudes (R Supercosmos) are given in Fig. 9 and Fig. 10, respectively.

4 BROWN DWARFS IN POSS I IMAGES

As pointed out in Sect. 3, most of the 298 165 candidates were discarded because they were detected in catalogues other than *Gaia* EDR3 or Pan-STARRS. Since most of the discarded sources were detected in the infrared, we looked into this sample to identify candidate brown dwarfs in POSS I images. This is relevant because it would imply that this class of objects was already recorded in photographic plates forty years before the confirmation of its first member (Rebolo et al. 1995).

For this, we made a spectral energy distribution fitting using VOSA and the BT-Settl CIFITS grid of model atmospheres (Baraffe et al. 2015). A candidate brown dwarf with effective temperature of 2 400 K (M9 V according to the Mamajek’s Color and Effective Temperature Sequence²⁰) was found. The SED fitting as well the position of the candidate brown dwarf in POSS I, 2MASS and Pan-STARRS images is shown in Fig. 11.

5 FAILED SUPERNOVAE?

In Villarroel et al. (2020b) the rate of failed supernovae was estimated to be less than 1 in 90 million during a 70 years of time window. We investigate the list of 298 165 transient sources to see if any of these can be found both in POSS I and in POSS II red images before vanishing. We find five candidates that each one turns out to be a superposition of a transient and artefact. Also, among the 5 399 final candidates, we found only two sources almost simultaneously observed in the POSS I blue and red images (the difference in observing time between the blue and red exposures is, typically, ~ 30 min). Although, on the basis of the displacements of the sources between the POSS I blue and red images, they could be classified as non-catalogued asteroids, the fact that the two sources show a point-like shape might question this hypothesis since, as mentioned in Sect. 3, asteroids are expected to show an elongated shape in the direction of the movement (Fig. 12). The small number of almost simultaneous transients in blue and red images can be, at least, partly explained by the different wavelength coverage (very red sources may not be visible in the blue, and viceversa) and by the different exposure times (typically, 45-60 min in the red and 8-10 min in the blue) which, despite some flux dilution due to the large observing time, makes higher the likelihood of finding a transient in red images.

The above results indicate that an entire disappearance of a star might be rare, which agrees with some theoretical predictions (Byrne & Fraser 2022). All-sky survey searches for failed supernovae are more likely to succeed on declining brightness of an object within $\Delta m < 3$ mag, rather than its entire disappearance. In order to reach a final conclusion on the rate of failed supernovae, a future study

²⁰ https://www.pas.rochester.edu/~emamajek/EEM_dwarf_UBVIJHK_colors_Teff.txt

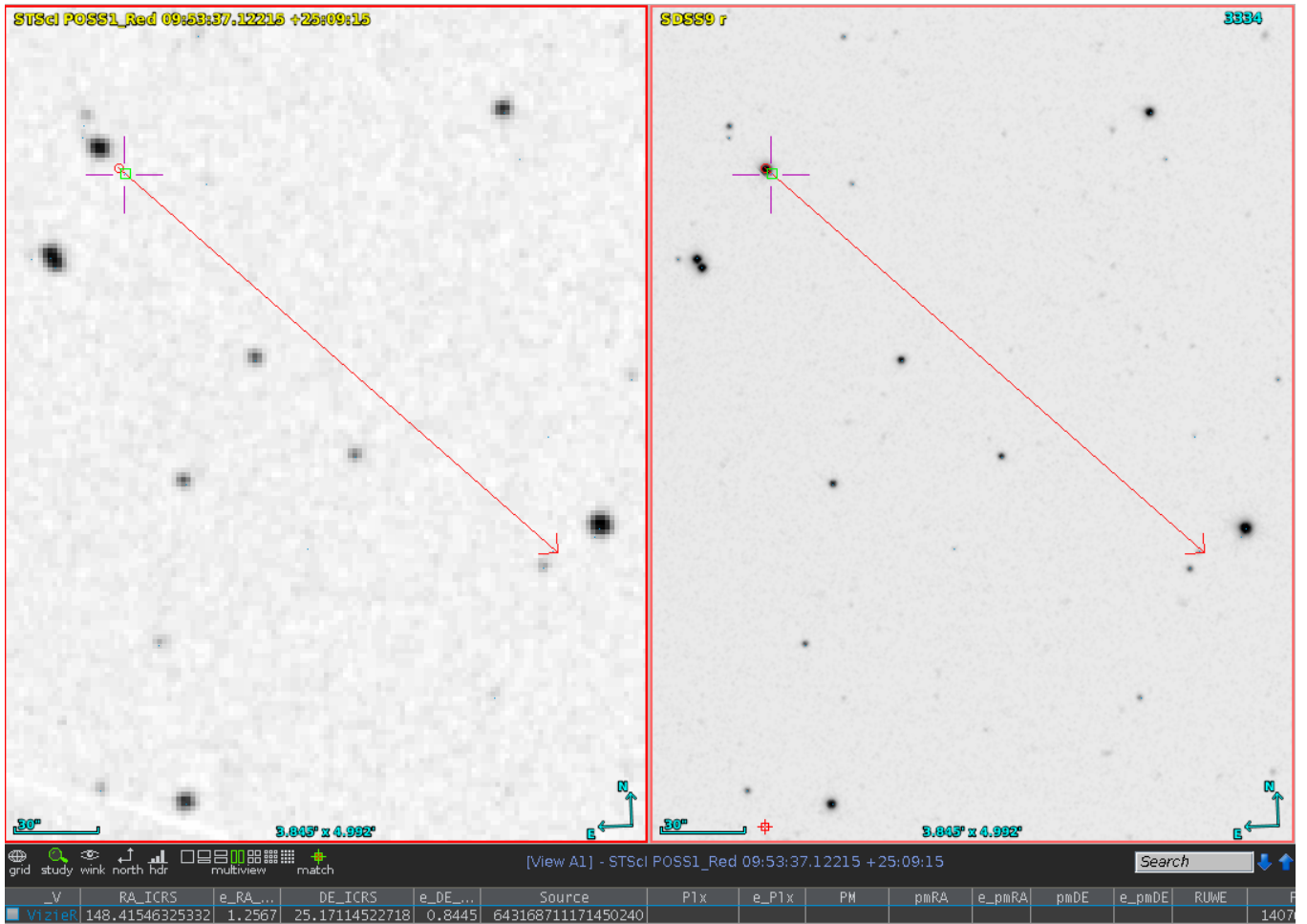


Figure 6. LP 371-1, the object marked with a cross in the SDSS image, is a high proper motion star as reported in Simbad (PMRA: -154 mas yr^{-1} ; PMDEC: -140 mas yr^{-1} ; red line) but without proper motion information in *Gaia* EDR3 (table shown at the bottom). See text for more details.

will carefully examine whether the complete list of 298,165 sources, as well as the list of candidates emerging from the VASCO citizen science project, contains candidates visible in both the blue and the red band.

6 SUMMARY

Working with three large-area sky surveys (POSS I, *Gaia* EDR3 and Pan-STARRS DR2) and a workflow based on Virtual Observatory archives and services, we have searched for sources identified in POSS I but not seen either in *Gaia* or Pan-STARRS finding 298 165 sources. After filtering sources found in other archives (mainly in the infrared), asteroids, high proper motion objects with no information on proper motion in *Gaia* EDR3, known variables and artefacts, we ended up with a list of 5 399 sources. Working with POSS I data has the advantage of getting rid from contamination of artificial satellites and, at the same time, opens the possibility of exploring long-term (of the order of decades) variability phenomena.

Although the origin of these 5 399 vanishing sources is not clear, most of them might be associated to large amplitude ($> 2.5 \text{ mag}$) variable stars like, for instance, flare stars. Other physical (unknown asteroids, non-catalogued high proper motion objects or exotic objects theoretically proposed like failed supernovae) and artificial (tech-

nosignatures) mechanisms can also be proposed to explain the disappearance of our list of objects in modern archives.

The candidates to vanishing stars 5 399 as well as the sources detected in the infrared but not in the visible (172 163) are easily accessible from a Virtual Observatory compliant archive. These sources can be of interest in searches for strong M-dwarf flares, extreme stellar variability on extended times-scales as well as extragalactic transients. Follow-up observations with bigger telescopes will reveal the presence/absence of an object in its place. Sources still missing after follow-up observations could also be useful for technosignature studies like, for instance, laser searches (Villarroel et al. 2020b; Marcy et al. 2022). The 298 165 sources will be further examined by the VASCO citizen science project (Villarroel et al. 2020a). Finally, it is also important to stress the fundamental role played by the Virtual Observatory in this paper. The discovery, access and analysis of millions of objects coming from tens of archives covering the electromagnetic spectrum from the ultraviolet to the mid-infrared would have not been possible without the tools and services provided by this e-infrastructure.

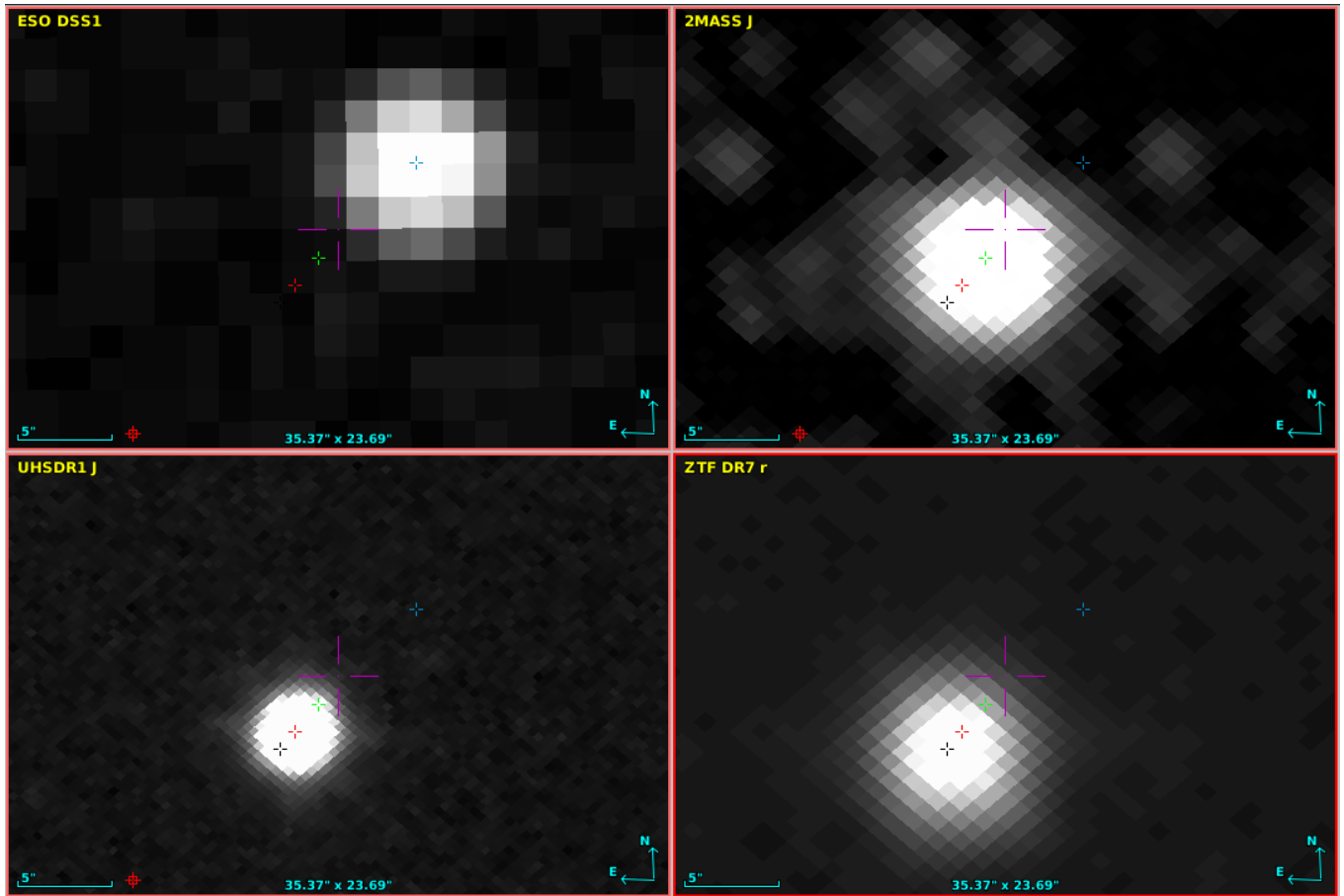


Figure 7. Example of a high proper motion object not reported either in *Gaia* EDR3 or Simbad. The blue/green/red/black crosses mark the position of the source in POSS I/2MASS/UKIDSS/ZTF images, respectively.

ACKNOWLEDGEMENTS

This research has made use of the Spanish Virtual Observatory (<https://svo.cab.inta-csic.es>) project funded by MCIN/AEI/10.13039/501100011033/ through grant PID2020-112949GB-I00 and MDM-2017-0737 at Centro de Astrobiología (CSIC-INTA), Unidad de Excelencia María de Maeztu. B.V. is funded by the Swedish Research Council (Vetenskapsrådet, grant no. 2017-06372) and is also supported by the The L'Oréal - UNESCO For Women in Science Sweden Prize with support of the Young Academy of Sweden. She is also supported by Märta och Erik Holmbergs donation.

This work presents results from the European Space Agency (ESA) space mission *Gaia*. *Gaia* data are being processed by the *Gaia* Data Processing and Analysis Consortium (DPAC). Funding for the DPAC is provided by national institutions, in particular the institutions participating in the *Gaia* MultiLateral Agreement (MLA). The *Gaia* mission website is <https://www.cosmos.esa.int/gaia>. The *Gaia* archive website is <https://archives.esac.esa.int/gaia>.

The Pan-STARRS1 Surveys (PS1) and the PS1 public science archive have been made possible through contributions by the Institute for Astronomy, the University of Hawaii, the Pan-STARRS Project Office, the Max-Planck Society and its participating institutes, the Max Planck Institute for Astronomy, Heidelberg and the Max Planck Institute for Extraterrestrial Physics, Garching, The Johns Hopkins University, Durham University, the University of

Edinburgh, the Queen's University Belfast, the Harvard-Smithsonian Center for Astrophysics, the Las Cumbres Observatory Global Telescope Network Incorporated, the National Central University of Taiwan, the Space Telescope Science Institute, the National Aeronautics and Space Administration under Grant No. NNX08AR22G issued through the Planetary Science Division of the NASA Science Mission Directorate, the National Science Foundation Grant No. AST-1238877, the University of Maryland, Eotvos Lorand University (ELTE), the Los Alamos National Laboratory, and the Gordon and Betty Moore Foundation.

This publication makes use of VOSA, developed under the Spanish Virtual Observatory project. This research has made use of Aladin (Bonnarel et al. 2000; Boch & Fernique 2014), Simbad (Wenger et al. 2000), and Vizier (Ochsenbein et al. 2000), developed at CDS, Strasbourg Observatory, France. TOPCAT (Taylor 2005) and STILTS (Taylor 2006) have also been widely used in this paper. This research has made use of the NASA/IPAC Infrared Science Archive, which is funded by the National Aeronautics and Space Administration and operated by the California Institute of Technology. This research has also made use of IMCCE's SkyBoT VO tool.

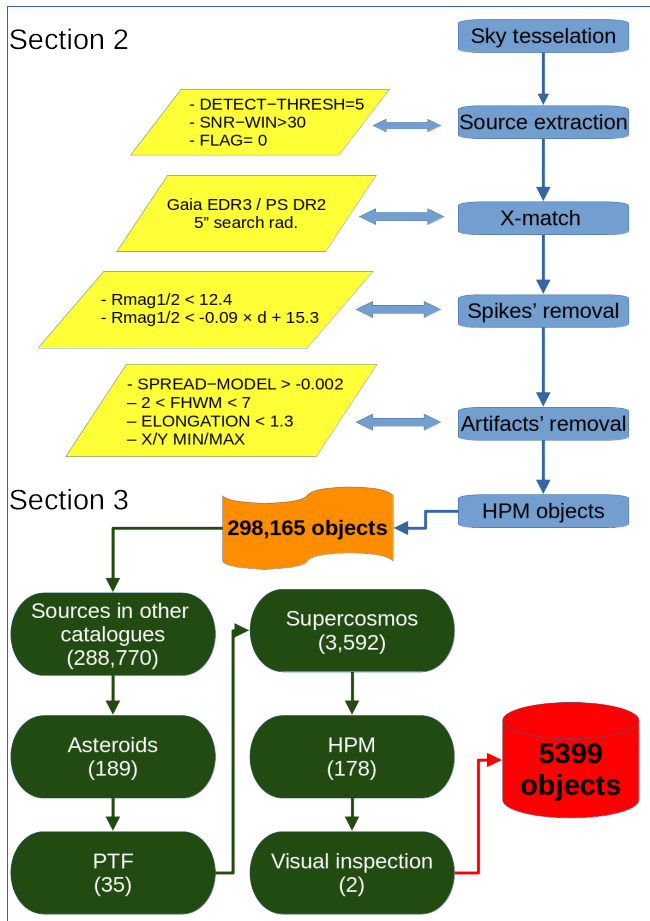


Figure 8. Flowchart of the candidate selection and analysis. See Sect. 2, and Sect. 3 for details.

7 DATA AVAILABILITY

The data underlying this article are available in the SVO archive of vanishing objects in POSS I red images available at <http://svocats.cab.inta-csic.es/vanish/>

REFERENCES

- Baraffe I., Homeier D., Allard F., Chabrier G., 2015, *A&A*, **577**, A42
- Bayo A., Rodrigo C., Barrado Y Navascués D., Solano E., Gutiérrez R., Morales-Calderón M., Allard F., 2008, *A&A*, **492**, 277
- Bellm E. C., et al., 2019, *PASP*, **131**, 018002
- Benson P. J., Clayton G. C., Garnavich P., Szkody P., 1994, *AJ*, **108**, 247
- Berthier J., Vachier F., Thuillot W., Fernique P., Ochsenein F., Genova F., Lainey V., Arlot J.-E., 2006, in Gabriel C., Arviset C., Ponz D., Enrique S., eds, *Astronomical Society of the Pacific Conference Series Vol. 351, Astronomical Data Analysis Software and Systems XV*. pp 367–+
- Bertin E., Arnouts S., 1996, *A&AS*, **117**, 393
- Boch T., Fernique P., 2014, in Manset N., Forshay P., eds, *Astronomical Society of the Pacific Conference Series Vol. 485, Astronomical Data Analysis Software and Systems XXIII*. p. 277
- Bonnarel F., et al., 2000, *A&AS*, **143**, 33
- Byrne R., Fraser M., 2022, arXiv e-prints, p. arXiv:2201.12187
- Cai Y. Z., et al., 2021, *A&A*, **654**, A157
- Cifuentes C., et al., 2020, *A&A*, **642**, A115
- Davenport J. R. A., 2019, arXiv e-prints, p. arXiv:1907.04443
- Gaia Collaboration et al., 2021, *A&A*, **649**, A1

- Greiner J., Motch C., 1995, *A&A*, **294**, 177
- Hartmann L., Kenyon S. J., 1996, *ARA&A*, **34**, 207
- Hilton E. J., West A. A., Hawley S. L., Kowalski A. F., 2010, *AJ*, **140**, 1402
- Izzo L., et al., 2019, *Nature*, **565**, 324
- Klagyivik P., Szabados L., 2009, *A&A*, **504**, 959
- Kochanek C. S., Beacom J. F., Kistler M. D., Prieto J. L., Stanek K. Z., Thompson T. A., Yüksel H., 2008, *ApJ*, **684**, 1336
- Kowalski A. F., Hawley S. L., Hilton E. J., Becker A. C., West A. A., Bochanski J. J., Sesar B., 2009, *AJ*, **138**, 633
- Lawrence A., et al., 2016, *MNRAS*, **463**, 296
- Leloudas G., et al., 2016, *Nature Astronomy*, **1**, 0002
- Marcy G. W., Tellis N. K., Wishnow E. H., 2022, *MNRAS*, **509**, 3798
- Minkowski R. L., Abell G. O., 1963, *The National Geographic Society-Palomar Observatory Sky Survey*. p. 481
- Monet D. G., et al., 2003, *AJ*, **125**, 984
- Nagoshi S., Iwamuro F., Wada K., Saito T., 2021, *PASJ*, **73**, 122
- Neustadt J. M. M., Kochanek C. S., Stanek K. Z., Basinger C., Jayasinghe T., Garling C. T., Adams S. M., Gerke J., 2021, *MNRAS*, **508**, 516
- Ochsenein F., Bauer P., Marcout J., 2000, *A&AS*, **143**, 23
- Pojmanski G., 1997, *Acta Astron.*, **47**, 467
- Rebolo R., Zapatero Osorio M. R., Martín E. L., 1995, *Nature*, **377**, 129
- Reid M. J., Goldston J. E., 2002, *ApJ*, **568**, 931
- Reynolds T. M., Fraser M., Gilmore G., 2015, *MNRAS*, **453**, 2885
- Tang S., Grindlay J., Los E., Laycock S., 2010, *ApJ*, **710**, L77
- Taylor M. B., 2005, in Shopbell P., Britton M., Ebert R., eds, *Astronomical Society of the Pacific Conference Series Vol. 347, Astronomical Data Analysis Software and Systems XIV*. p. 29
- Taylor M. B., 2006, in Gabriel C., Arviset C., Ponz D., Enrique S., eds, *Astronomical Society of the Pacific Conference Series Vol. 351, Astronomical Data Analysis Software and Systems XV*. p. 666
- Udalski A., Szymański M. K., Szymański G., 2015, *Acta Astron.*, **65**, 1
- Urban S. E., Corbin T. E., Wycoff G. L., Martin J. C., Jackson E. S., Zacharias M. I., Hall D. M., 1998, *AJ*, **115**, 1212
- Villarroel B., Imaz I., Bergstedt J., 2016, *AJ*, **152**, 76
- Villarroel B., et al., 2020a, arXiv e-prints, p. arXiv:2009.10813
- Villarroel B., et al., 2020b, *AJ*, **159**, 8
- Villarroel B., Mattsson L., Guergouri H., Solano E., Geier S., Dom O. N., Ward M. J., 2022, *Acta Astronautica*, **194**, 106
- Watson C. L., Henden A. A., Price A., 2006, *Society for Astronomical Sciences Annual Symposium*, **25**, 47
- Wenger M., et al., 2000, *A&AS*, **143**, 9
- de Ruyter S., van Winckel H., Dominik C., Waters L. B. F. M., Dejonghe H., 2005, *A&A*, **435**, 161
- van Genderen A. M., 2001, *A&A*, **366**, 508

APPENDIX A: VIRTUAL OBSERVATORY COMPLIANT, ONLINE CATALOGUE

In order to help the astronomical community on using our catalogue of candidates to vanishing objects, we developed an archive system that can be accessed from a webpage²¹ or through a Virtual Observatory ConeSearch.²²

The archive system implements a very simple search interface that allows queries by coordinates and radius as well as by other parameters of interest. The user can also select the maximum number of sources (with values from 10 to unlimited). The result of the query is a HTML table with all the sources found in the archive fulfilling the search criteria. The result can also be downloaded as a VOTable or a CSV file. Detailed information on the output fields can be obtained placing the mouse over the question mark located close to the name

²¹ <http://svocats.cab.inta-csic.es/vanish/>

²² for instance, <http://svocats.cab.inta-csic.es/vanish-poss/ps.php?RA=0.708&DEC=47.155&SR=0.1&VERB=2>

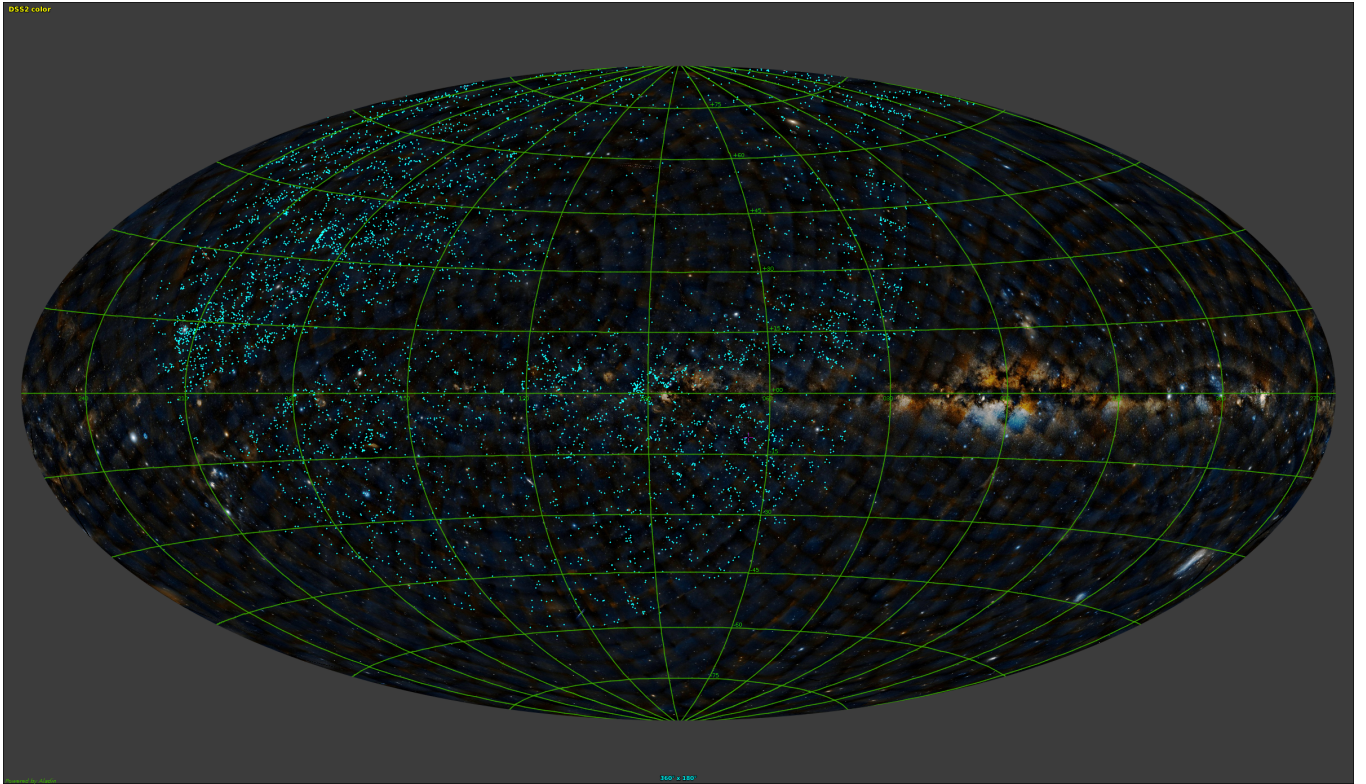


Figure 9. Spatial distribution in galactic coordinates of the final list of 5 399 candidates (blue dots). A coloured POSS-II images is displayed in the background.

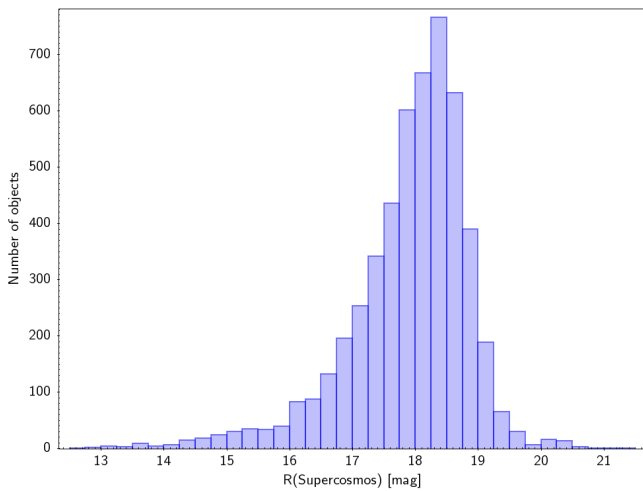


Figure 10. Distribution of the SuperCOSMOS R magnitudes of the final sample (5 399 objects). It peaks at $R \sim 18,5$ with 80 % of the target with magnitudes in the range $17 \leq R \leq 19$.

of the column. The archive also implements the SAMP²³ (Simple Application Messaging) Virtual Observatory protocol. SAMP allows Virtual Observatory applications to communicate with each other in a seamless and transparent manner for the user. This way, the results

of a query can be easily transferred to other VO applications, such as, for instance, Topcat.

This paper has been typeset from a $\text{\TeX}/\text{\LaTeX}$ file prepared by the author.

²³ <http://www.ivoa.net/documents/SAMP>

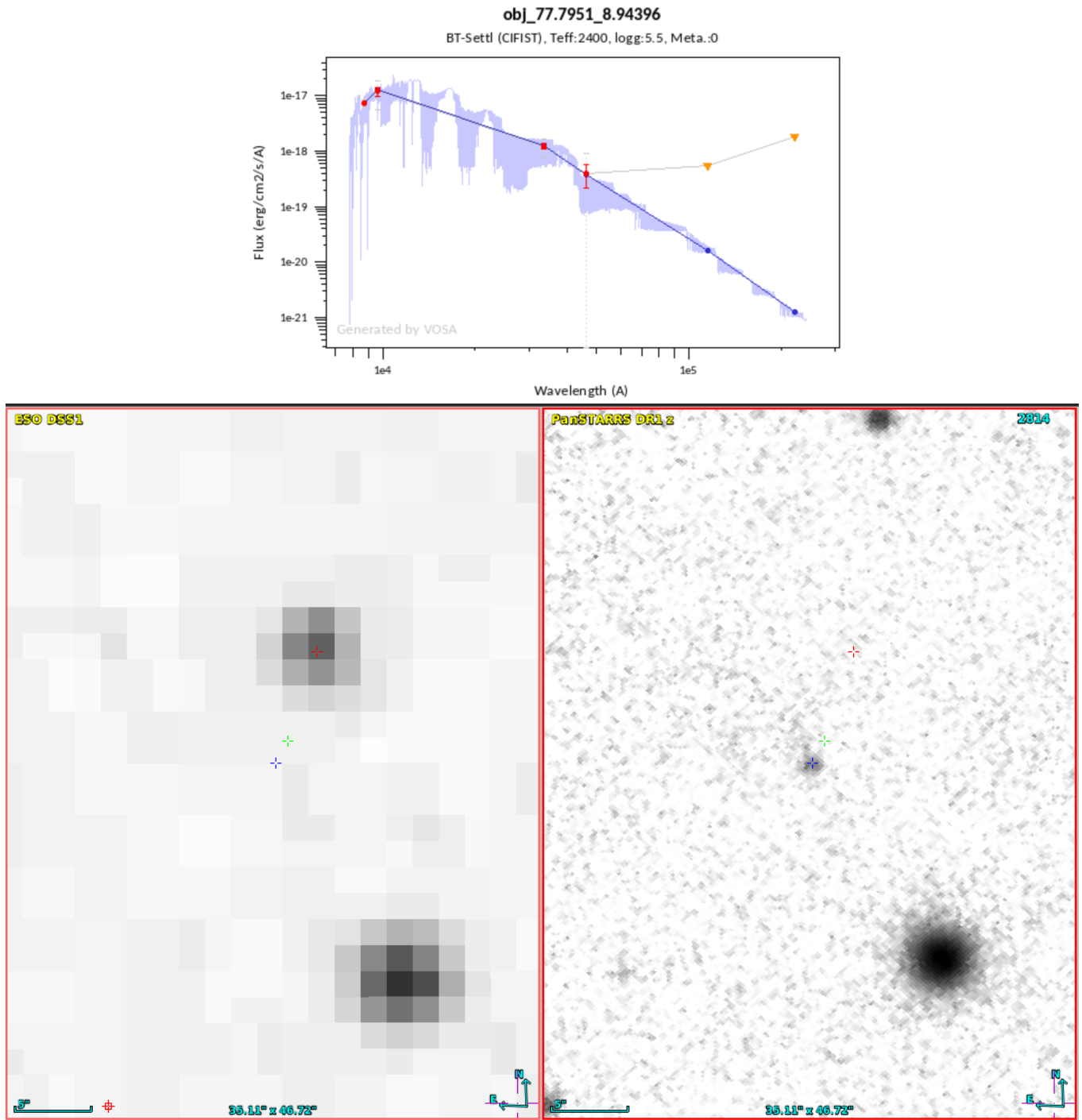


Figure 11. Top: Spectral energy distribution fitting of the candidate brown dwarf (RA: 77°.7951, DEC: 8°.94396). The red dots represent the observed photometry. Overplotted in blue is the best fitting CIFIST model. Photometric upper limits are plotted as inverted yellow triangles and are not considered in the SED fitting process. **Bottom:** The candidate brown dwarf as seen in POSS I (red cross) and Pan-STARRS (blue cross). The green cross in between indicates the position of the source in an intermediate epoch (2MASS).

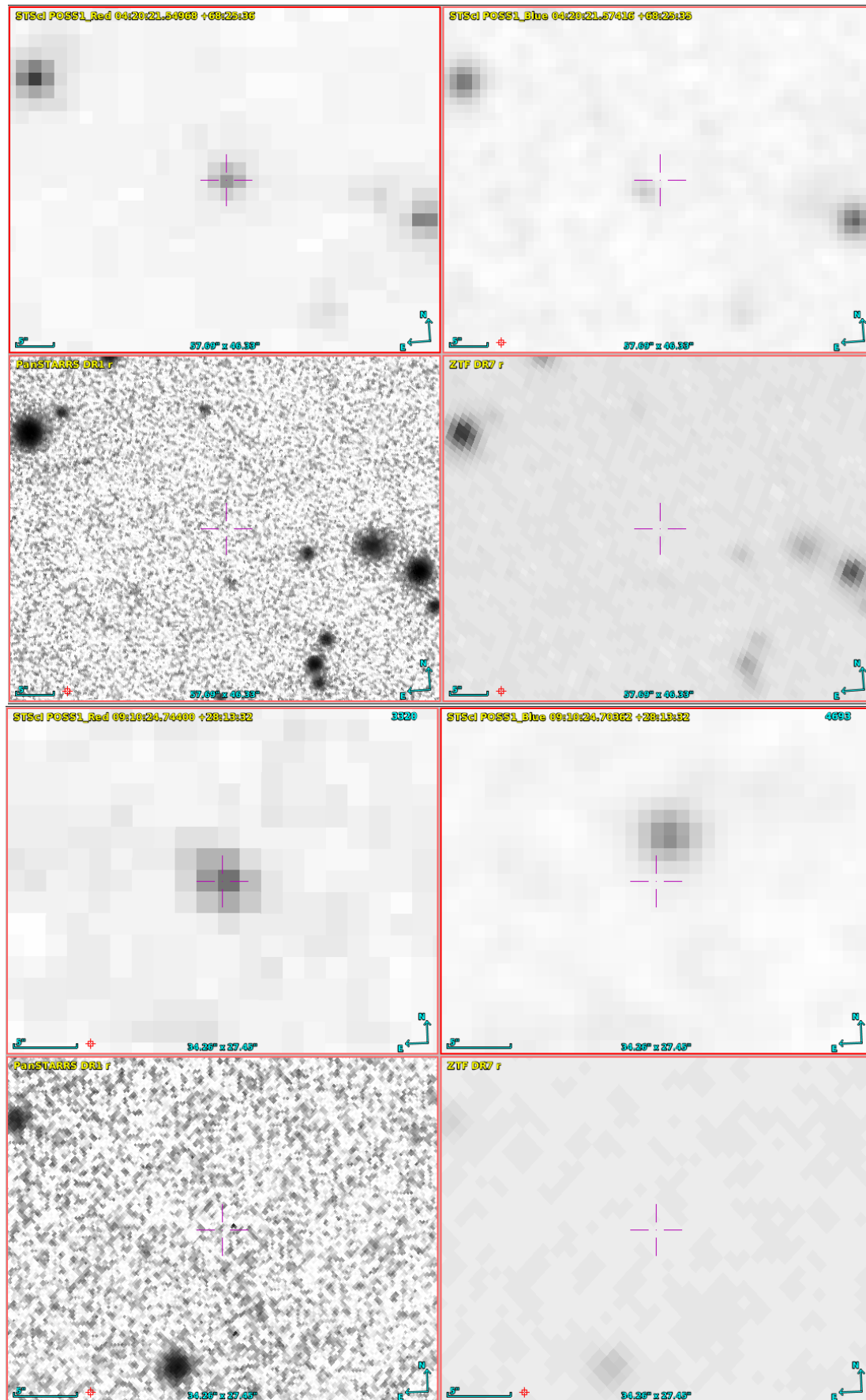


Figure 12. Two sources seen in POSS I red and blue images (differences in time ~ 30 min) but not detected in more recent surveys.